Title:

Mitigating nitrous oxide emission by an ultra-fast bioprocess enabling the removal of high concentration N_2O

Authors:

Ryota Maeda[1], Mikiko Sato[1], Kiwamu Minamisawa[2] and Kengo Kubota[1,3,*]

Affiliations:

[1] Department of Frontier Sciences for Advanced Environment, Graduate School of Environmental Studies, Tohoku University, 6-6-06 Aza-Aoba, Aramaki, Aoba-ku, Sendai, Miyagi 980-8579, Japan

[2] Department of Ecological Developmental Adaptability Life Sciences, Graduate School of Life Science, Tohoku University, 2-1-1 Katahira, Aoba-ku, Sendai, 980-18577, Japan

[3] Department of Civil and Environmental Engineering, Graduate School of Engineering, Tohoku University, 6-6-06 Aza-Aoba, Aramaki, Aoba-ku, Sendai, Miyagi 980-8579, Japan

Corresponding Author:

*Kengo Kubota

Department of Frontier Sciences for Advanced Environment, Graduate School of Environmental Studies, Tohoku University, 6-6-06 Aoba, Aramaki, Aoba-ku, Sendai, Miyagi 980-8579, Japan.

Tel. & Fax: +81-22-795-5011

E-mail: kengo.kubota.a7@tohoku.ac.jp

Abstract

Nitrous oxide (N_2O) is known as a greenhouse gas as well as an ozone-depleting substance. Wastewater treatment process is one of the sources of N_2O emission, and the high concentrations of N_2O in off-gas were reported from an anaerobic ammonium oxidation process. This study developed a novel N_2O removal process using a down-flow hanging sponge reactor to remove high concentrations of N_2O. More than 96% removal efficiencies were achieved for up to 300 ppm N_2O with 3 min gas retention time (GRT), and more than 99% removal efficiency was obtained for 2,000 ppm N_2O with 18 min GRT. A maximum removal rate of 161 ± 26 mg-N/L-reactor/day was achieved, that was over 10 times faster than the pioneering process. Kinetic analysis indicated that the N_2O dissolution rate is a crucial factor in determining the N_2O removal rate in the reactor. Various N_2O reducers were detected in reactors, and *Azonexus* was thought to play a key role. Most of the *nosZ* genes obtained belonged to clade I and only a few clade II *nosZ* genes were retrieved.

Keywords:

Down-flow hanging sponge (DHS); kinetics; metagenome; microelectrode; nitrous oxide (N_2O); *nosZ* gene; 16S rRNA gene amplicon

1. Introduction

Nitrous oxide (N_2O) is a greenhouse gas and an ozone-depleting substance (Ravishankara et al., 2009). Its atmospheric concentration has increased significantly over the last 100 years, reaching 336 ppb in 2022 (IPCC, 2022; Tian et al., 2020). N_2O has approximately 273 times greater global warming potential than that CO_2 and has a lifetime of 114 years in the atmosphere. The recent increase in N_2O emissions exceeds the worst-emission scenario of the IPCC; therefore, the reduction of N_2O emissions is an urgent issue globally (Tian et al., 2020). The agricultural sector is the main source of N_2O emissions, accounting for more than half of human activity-related emissions. Although their contribution is much lower, the waste and wastewater treatment sectors are also sources of N_2O.

In wastewater treatment, N_2O is generated in both aerobic and anaerobic processes related to nitrogen removal (i.e. nitrification and denitrification) by biotic and abiotic transformation processes (e.g. nitrifier denitrification, hydroxylamine oxidation, and incomplete denitrification) (Hallin et al., 2018; Sabba et al., 2018). Earlier studies identified several factors that influence N_2O generation from wastewater treatment processes (e.g. dissolved oxygen (DO), nitrite and ammonium concentrations, and the chemical oxygen demand (COD) /N ratio) (Domingo-Félez and Smets, 2019; Kampschreur et al. 2009; Vasilaki et al. 2019; Wu et al. 2020). N_2O emission mitigation approaches, such as DO control (Duan et al., 2021) and COD/N ratio control through carbon source input (Hu et al., 2013; Peng et al., 2017) were reported. However, these approaches are not necessarily universal because they are only effective under specific conditions (Han et al., 2023; Oba et al., 2024). As an alternative approach, processes removing N_2O in off-gas using microbial reactions were developed (e.g., utilising a fixed bed reactor packed with Kaldnes rings (Frutos et al., 2016) or biofilters filled with polyurethane foam (Han et al., 2023; Yoon et al., 2019,

69 2017)). These studies targeted 100–300 ppm of N_2O in either N_2 (anaerobic) or air (aerobic)
70 and successfully reduced N_2O in the gaseous phase.

71 In addition to conventional nitrification-denitrification processes, anaerobic
72 ammonium oxidation (anammox) is being considered for the removal of nitrogen from
73 wastewater. More than 100 anammox-based full-scale plants are used globally to treat
74 industrial and municipal wastewater (Lackner et al., 2014). The generation of N_2O from
75 anoxic anammox tanks were reported (Ali et al., 2016; Kampschreur et al., 2009, 2008;
76 Okabe et al., 2011; Vasilaki et al., 2019) with concentrations reaching 1,300 ppm
77 (laboratory-scale) (Okabe et al., 2011) and 4,000 ppm (full-scale) (Kampschreur et al., 2008)
78 in off-gas, which is much higher than that of the previously tested concentrations for N_2O
79 removal (200 ppm in N_2) (Yoon et al., 2017).

80 To remove high concentrations of N_2O generated from anaerobic/anoxic wastewater
81 treatment processes, such as anammox processes, we focused on down-flow hanging sponge
82 (DHS) processes. DHS was originally developed for wastewater treatment, maintaining high
83 sludge biomass in sponge media and resulting in effluent water quality comparable to that of
84 conventional activated sludge processes. It allows aerobic treatment without aeration by
85 supplying oxygen from the air due to gas-liquid equilibrium, while wastewater flows from top
86 to bottom due to gravity (Kubota et al., 2024). The application of DHS reactors for gaseous
87 substances such as hydrogen sulfide and toluene were reported by using the closed reactors
88 (Tanikawa et al., 2022; Yamaguchi et al., 2018).

89 In this study, we developed a process that rapidly removed high concentrations of N_2O
90 using DHS. The N_2O removal performance of the DHS reactors was evaluated by feeding
91 different concentrations of N_2O (5–2,000ppm) and supplying the supernatant from an
92 anaerobic sewage sludge digester as a carbon source. Microelectrode experiments were
93 conducted to assess the kinetics of the N_2O reduction. Eventually, the microorganisms that

may be involved in N_2O removal were identified using 16S rRNA gene amplicon and shotgun metagenome analyses.

2. Material and Methods

2.1 Reactor configuration and operation

A DHS reactor consisting of fifteen sponge carriers with polyethene plastic net rings was placed in a closed column with a volume of 1.23 L. The carriers were vertically connected and suspended in the column. The size of polyurethane sponge was 30 mm in diameter and 30 mm in height. The total sponge volume was 0.32 L, resulting in a packing density of 26%.

Anaerobic sludge obtained from an anaerobic digester treating sewage sludge under mesophilic conditions was used as the seed sludge. The supernatant of the digested sludge was used as a carbon source and fed from the top of the reactor with a hydraulic retention time (HRT) of 3–24 hours based on the sponge volume. Feeding was performed intermittently using a timer. N_2 gas containing 5, 40, 300 or 2,000 ppm N_2O was subjected to the closed column from the inlet near the bottom of the reactor. The outlet for the treated gas was placed near the top of the reactor, resulting in gas flow from the bottom to the top. The gas flow rate was adjusted using a gas meter (RK1200; KOFLOC, Kyoto, Japan). The gas retention time (GRT) was adjusted by varying the gas flow rate. The reactor was set in an incubation chamber and operated anaerobically at 25ºC in the dark. The GRT was calculated by using a gas volume at 25ºC and an effective reaction volume of 0.91 L. Nitrogen loading of the reactor was calculated by using a reactor volume of 1.23 L and the amount of nitrogen under the standard temperature (0ºC). A schematic of the experiment is shown in Fig.1.

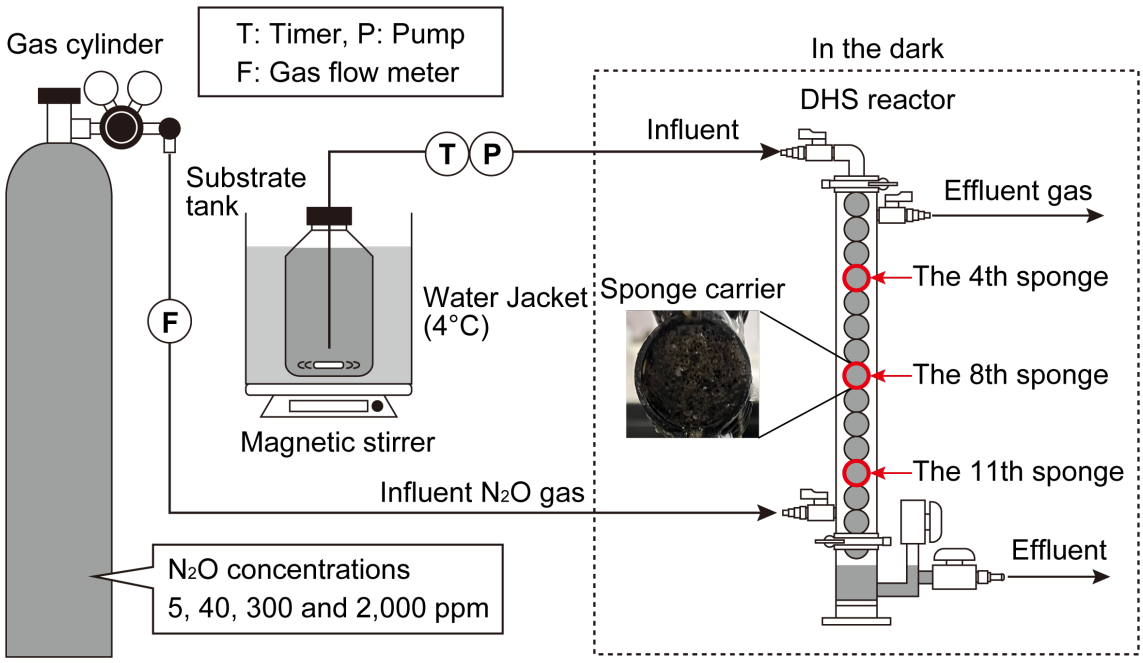

Fig. 1. Schematic diagram of the experiment. The sludge samples collected from the 4th, 8th and 11th sponges from the top were used for the microelectrode experiments. The 4th and 11th sponges were used for 16S rRNA amplicon and metagenome analyses.

2.2 Measurement of gaseous N_2O concentration

The effluent gas from the closed DHS reactor was measured every 1–2 days to evaluate N_2O removal performance. In this study, two sets of electron capture detector gas chromatography (ECD-GC) (GC-2014, Shimadzu, Kyoto, Japan) with different columns were used, depending on the N_2O concentration. Both ECD-GCs were equipped with a 63Ni ECD, and N_2 was used as the carrier gas. For the measurement of lower N_2O concentrations (< approximately 40 ppm), an ECD-GC with a tandem Porapak Q column (80/100 mesh; 3.0 mm × 1.0 m and 3.0 mm × 2.0 m, GL Sciences, Japan) was used. The temperatures were set at 80°C, 100°C, and 340°C for the column, injector, and detector, respectively. For the measurement of higher N_2O concentrations (> approximately 40 ppm), an ECD-GC with a TC-BOND Q column (0.53 mm × 30 m, df=20 μm, GL Sciences, Japan) was used. The

133 temperatures were set at 50°C, 280°C, and 300°C for the column, injector, and detector,
134 respectively.
135
136 **2.3 Water quality analysis and sludge sampling**
137 Influent water and effluent water from the DHS reactor were sampled to evaluate
138 changes in water quality. COD was measured using a HACH water quality analyser (DR890,
139 HACH, Loveland, CO, USA).
140 Sludge samples were collected on the final experimental day. A sponge was immersed
141 in 0.05 × phosphate buffered saline (PBS; 130 mM NaCl, 10.8 mM Na_2HPO_4, 4.2 mM
142 NaH_2PO_4, pH 7.4) in a plastic bag, and sludge was suspended in PBS by squeezing the
143 sponges. Part of the suspended sludge was used for microelectrode experiments (see Section
144 2.4). The other part was centrifuged at 2935×g for 15 min at 4°C. After removing the
145 supernatant, a portion of the sludge was stored at -20°C for DNA extraction. The other part
146 was used to measure the suspended solids (SS) and volatile suspended solids (VSS) according
147 to the standard methods (APHA, 2017).
148
149 **2.4 Microelectrode experiment for measuring N_2O consumption rate**
150 The N_2O consumption rates of the sludge samples were measured using an N_2O
151 micro-respiration system with amperometric microsensors (Unisense, Aarhus, Denmark) (Fig.
152 S1). Measurements and subsequent data analyses were conducted in accordance with an
153 earlier study (Suenaga et al., 2018). Briefly, the sludge samples collected from the 4th, 8th
154 and 11th sponges (Fig. 1) were used for the experiments. The sludge samples were initially
155 diluted with anaerobic sludge digester supernatant, which was filter sterilised by using 0.22
156 μm Stericup® filter (S2GVU01RE, Merck Millipore, Germany) to make sludge concentration
157 suitable for the microelectrode experiment. Approximately 8 ml double-port chamber
158 (Unisense, Aarhus, Denmark) was filled with the sample and placed in a water bath controlled

159 at 25°C. N_2O sensors were inserted into the chamber, and a certain amount (30–40 μl) of N_2O
160 water prepared by aerating pure N_2O gas was injected into the chamber using a Hamilton
161 syringe. The sample was stirred at 600 rpm, and the N_2O concentration was continuously
162 recorded using SensorTrace Suite ver. 2.8.0 (Unisense). After the injected N_2O was
163 completely consumed, fresh N_2O water was injected, and N_2O consumption was measured.
164 For the data analysis, noise removal and plot smoothing were performed using Sigma
165 Plot 13.0 (Systat Software, San Jose, CA, USA). The theoretical maximum consumption rate
166 of N_2O (V_{max}) was obtained using the Michaelis-Menten equation and the Excel solver
167 function (Suenaga et al., 2018). The theoretical maximum N_2O removal rate per reactor
168 volume (mg-N/L-reactor/day) was calculated by multiplying V_{max} (N_2O removal rate per
169 VSS) by the amount of VSS in the reactor.
170
171 **2.5 16S rRNA gene amplicon sequence analysis**
172 Sludge samples collected from the 4th and 11th sponges of each reactor were
173 subjected to 16S rRNA gene amplicon sequencing analysis. DNA extraction was performed
174 using ISOIL for Beads Beating kits (Nippon Gene, Tokyo, Japan), according to the
175 manufacturer's instructions. Prokaryotic 16S rRNA genes were amplified using 341f
176 (5'-CCTAYGGGGRBGCASCAG-3') and 806r mix (806r (5'-
177 GGACTACHVGGGGTHTCTAAT-3') and 806r-P (GGACTACCAGGGTATCTAAG-3') in
178 a 30:1 ratio) (Matsubayashi et al., 2017). The PCR conditions for library preparation were as
179 described earlier (Ni et al., 2020). 16S rRNA gene amplicon sequencing using the MiSeq
180 Reagent Kit v3 600 cycles was outsourced to the Bioengineering Lab. Co., Ltd. (Kanagawa,
181 Japan). Nucleotide sequence data are available in the DDBJ Sequence Read Archive
182 accession number PRJDB18886.
183 Data analysis was conducted using QIIME2 ver. 2023.7 (Bolyen et al., 2019).
184 Quality trimming, primer sequence removal, paired-end assembly, and chimaera checking of

185 the raw 16S rRNA gene sequencing data were performed using DADA2 (Callahan et al.,
186 2016). The 16S rRNA gene sequences with ≥ 97% identity were clustered into operational
187 taxonomic units (OTUs) using VSEAECH (Rognes et al., 2016). The OTUs were classified
188 using the Greengens2 database (McDonald et al., 2023).
189
190 **2.6 Shotgun metagenome analysis**
191 DNA extracted from the 4th and 11th sponges in each reactor was subjected to
192 short-read metagenomic analysis. Library preparation and sequencing were outsourced to the
193 Bioengineering Lab. Co., Ltd.. In brief, sequencing libraries were prepared using the
194 MGIEasy FS DNA Library Prep Set (MGI Tech, Shenzhen, China) and 150 bp paired-end
195 reads were generated using DNBSEQ-G400 (MGI Tech). Nucleotide sequence data are
196 available in the DDBJ Sequence Read Archive accession number PRJDB18886.
197 The generated reads were subjected to SOAPnuke 2.0.6 (Chen et al., 2018) to
198 remove the adaptor sequences and low-quality reads. Assembly was performed using the
199 workflow “aviary assemble” in Aviary 0.8.3 (Newell et al., 2023). Contigs shorter than 600
200 bp were excluded from subsequent analyses. Contigs containing putative *nosZ* gene sequences
201 were retrieved using the BLASTN algorithm (Altschul et al., 1990) and a *nosZ* database
202 (Zheng et al., 2023). The coverage of contigs was analysed coverM 0.7.0 (Aroney et al.,
203 2024), and the relative abundance of each *nosZ* gene was calculated. The obtained contigs
204 were subjected to the workflow "aviary annotate" and Prokka 1.14.6 (Seemann, 2014) for
205 functional annotation. Eventually, contigs containing NosZ protein sequences with ≥ 300
206 amino acids were extracted to construct a phylogenetic tree.
207 A phylogenetic tree of the NosZ sequences obtained in this study was constructed using
208 known reference NosZ sequences. The reference sequences were obtained by clustering the
209 *nosZ* gene sequences (Zheng et al., 2023) with 70% sequence identity using VSEARCH
210 2.27.0. The reference sequences (n=574) were converted to amino acid sequences. The amino

211 acid sequences were aligned using MAFFT (Katoh et al., 2002) and trimmed using TrimAl
212 (Capella-Gutiérrez et al., 2009). A phylogenetic tree was constructed using IQ-tree2 (Minh et
213 al., 2020). The best-fit model was LG + F + R10, as determined using ModelFinder
214 (Kalyaanamoorthy et al., 2017). The phylogenetic tree was visualised using iTOL v6 (Letunic
215 and Bork, 2021).
216
217 **3. Results**
218 **3.1 N_2O removal performance by DHS reactors**
219 In this study, the continuous treatment of gaseous N_2O was conducted using DHS
220 reactors. The N_2O removal performance was evaluated using different concentrations of N_2O
221 in N_2 (5, 40, 300 and 2,000 ppm) under various N_2O loads by changing the gas flow rates
222 (shortest GRT of 3 min) (Fig. 2 and Tables S1 and S2). Hereafter, each reactor is denoted as 5,
223 40, 300, and 2,000 ppm N_2O reactor.
224 The 5 ppm N_2O reactor (Fig. 2a and Table S1) started with a GRT of 18 min. The N_2O
225 removal efficiency reached over 90% after one day, and high removal performance was kept
226 even at a GRT of 9.1 and 4.6 min. Finally, the removal efficiency of 97 ± 5.4% was obtained
227 under the GRT of 3.0 min with the N_2O removal rate of 2.0 ± 0.1 mg-N/L-reactor/day.
228 The 40 ppm N_2O reactor (Fig. 2b, Table S1) also showed high removal efficiency after
229 starting up, showing 95 ± 3.9% and 99 ± 0.9% removal efficiency under the GRT of 18 min
230 and 9.1 min by day 20, respectively. When the GRT was shortened to 6.1 min, the removal
231 efficiency dropped to 74 ± 17% (days 20–50) due to insufficient COD supply (Fig. 2b and
232 Tables S1 & S2). After supplying sufficient COD, N_2O removal became stable with the
233 removal efficiency of 96 ± 3.4% under the GRT of 3.6 min (days 71–85, removal rate; 13 ±
234 0.5 mg-N/L-reactor/day).
235 The N_2O removal performance of the 300 ppm N_2O reactor (Fig. 2c and Table S1) was
236 similar to the 40 ppm N_2O reactor. Over 99% removal efficiency was obtained under the GRT

as short as 6.1 min (days 61–70), except for the term of days 20–50, during which the COD supply was deficient, and the removal efficiency dropped to 39 ± 16%. On day 70, reactor operation was stopped for unavoidable reasons (Fig. 2c). After a few weeks of suspension, the reactor was restarted with new sponges and seed sludge by feeding 300 ppm N_2O gas with a GRT of 6.1 min (the day of re-start-up was set as day 71 for convenience). An N_2O removal rate of over 97% was achieved after four days of operation. The GRT was further shortened to 3.0 min, resulting in the N_2O removal efficiency of 94 ± 1.5% (days 108–117, removal rate; 113 ± 1.8 mg-N/L-reactor/day).

The 2,000 ppm N_2O reactor (Fig. 2d and Table S1) was initially operated at a GRT of 18 min. The removal efficiency in the first week was only 57 ± 1.5%; therefore, the GRT was extended to 36 min, resulting in the removal efficiency of 98 ± 6.7%. The GRT was set at 18 min again, and low removal efficiency of 36 ± 18% was observed because of insufficient COD supply (days 20–50) (Fig. 2d and Tables S1 and S2). High removal efficiency of 99 ± 0.6% was achieved with increased organic loading rate (days 61–70). The reactor was stopped after 70 days of operation. Similar to the 300 ppm N_2O reactor, new seed sludge was inoculated, and the reactor was restarted with a GRT of 18 min. The removal efficiency reached ≥ 99% again after 12 days of operation, and the stable and high removal efficiency of 99 ± 0.1% was observed on days 83–86 (removal rate; 132 ± 0.1 mg-N/L-reactor/day) (Fig. 2d and Table S1). High removal efficiency was not achieved even under higher organic loading rate at the GRT of 9.1 min. Lower N_2O removal efficiency of 61 ± 10% was obtained (days 87–119), but the highest N_2O removal rate of 161 ± 26 mg-N/L-reactor/day was achieved in this period.

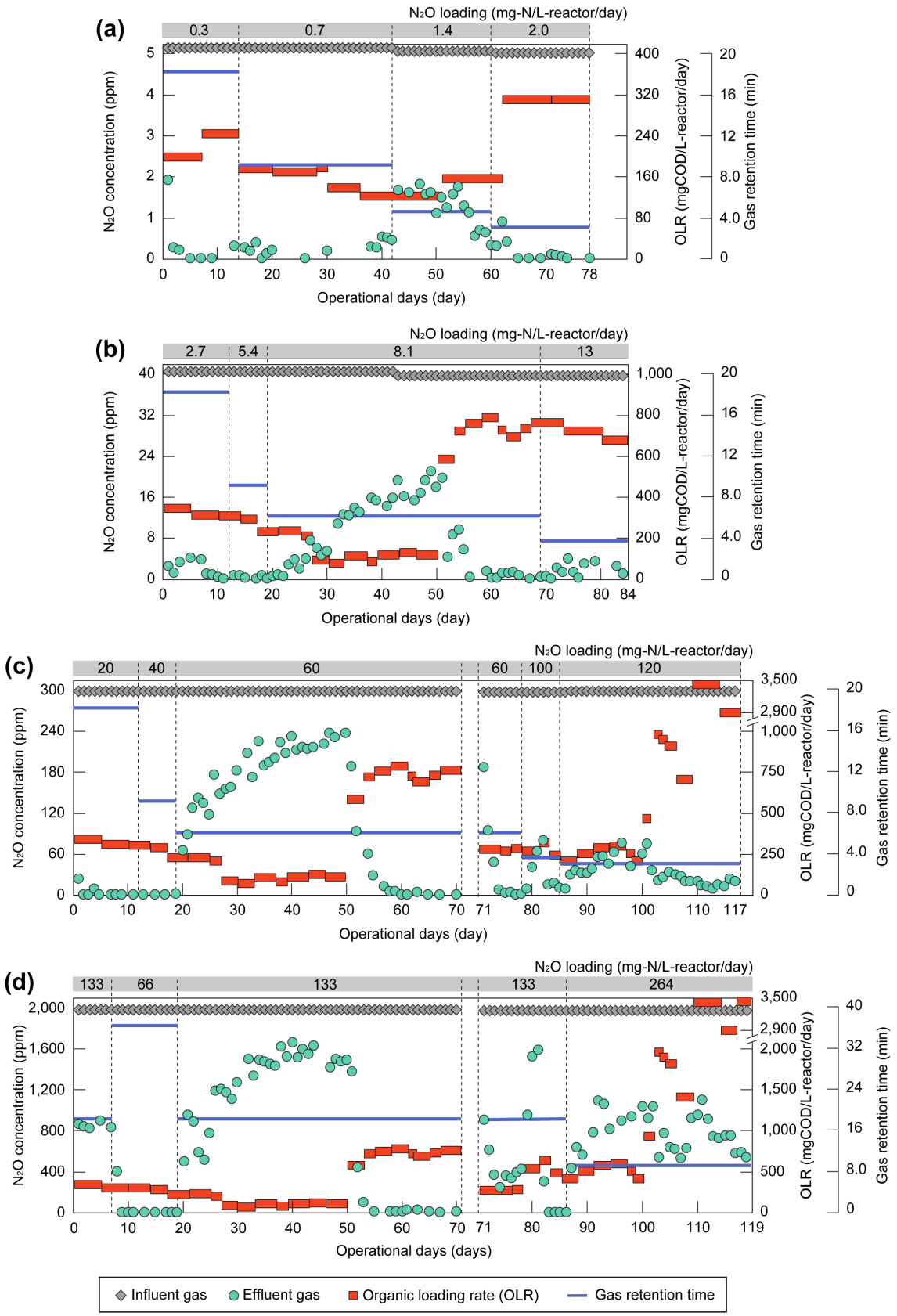
(a)
N2O loading (mg-N/L-reactor/day)
0.3
0.7
1.4
2.0
N2O concentration (ppm)
OLR (mgCOD/L-reactor/day)
Gas retention time (min)
Operational days (day)
(b)
N2O loading (mg-N/L-reactor/day)
2.7
5.4
8.1
13
N2O concentration (ppm)
OLR (mgCOD/L-reactor/day)
Gas retention time (min)
Operational days (day)
(c)
N2O loading (mg-N/L-reactor/day)
20
40
60
60
100
120
N2O concentration (ppm)
OLR (mgCOD/L-reactor/day)
Gas retention time (min)
Operational days (day)
(d)
N2O loading (mg-N/L-reactor/day)
133
66
133
133
264
N2O concentration (ppm)
OLR (mgCOD/L-reactor/day)
Gas retention time (min)
Operational days (days)
Influent gas
Effluent gas
Organic loading rate (OLR)
Gas retention time

261 Fig. 2. Nitrous oxide (N_2O) removal performance. Different concentrations of N_2O in
262 nitrogen gas were treated under different gas retention times and organic loadings. a; 5 ppm
263 N_2O, b; 40 ppm N_2O, c; 300 ppm N_2O, d; 2,000 ppm N_2O.
264
265 **3.2 N_2O consumption rate**
266 The N_2O consumption rates of the sludge collected from the 300 ppm and 2,000 ppm
267 N_2O reactors were measured using microelectrodes, as described earlier (Suenaga et al. 2018)
268 (Fig. S1). Theoretical maximum N_2O removal rates calculated using the Michaelis-Menten
269 equation were 1,189 ± 257 mg-N/L-reactor/day and 1,468 ± 186 mg-N/L-reactor/day at the
270 300 ppm and 2,000 ppm N_2O reactor, respectively (Table 1). Simultaneously, the actual
271 highest N_2O consumption rates of the reactors were 113 ± 1.8 mg-N/L-reactor/day (days
272 108–117 for the 300 ppm N_2O reactor) and 161 ± 26 mg-N/L-reactor/day (days 102–119 for
273 the 2,000 ppm N_2O reactor). These values were approximately 10% of the theoretical
274 maximum N_2O consumption rate.
275
276 Table 1. Nitrous oxide removal rates.

Reactor	Maximum N_2O removal rate of the reactor (mg-N/L-reactor/day)	The calculated theoretical N_2O removal rate (based on the Michaelis–Menten equation) (mg-N/L-reactor/day) [a]
300 ppm N_2O	113 ± 1.8 (days 108–117)	1,189 ± 257
2,000 ppm N_2O	161 ± 26 (days 102–119)	1,468 ± 186

277 [a] N_2O removal rate per reactor volume was calculated based on the amount of volatile
278 suspended solids retained in the reactor.
279
280 **3.3 Microbial community involved in N_2O reduction**
281 **3.3.1 16S rRNA gene amplicon analysis**

282 The microbial communities of the sludge samples evaluated by 16S rRNA gene
283 amplicon analysis are shown in Table S3, and the top 30 OTUs with average relative
284 abundances are summarised in Fig. 3. The microbial communities built in the reactors
285 differed from those in the seed sludge and substrate, as demonstrated by principal coordinate
286 analysis (PCoA) (Fig. S2). The microbial community structures changed with N_2O
287 concentrations and along the height of the reactors, although the N_2O concentrations had the
288 greatest effect.

289 Some OTUs with high relative abundance were similar to known N_2O-reducing
290 microorganisms (Fig. 3). OTU0001, which is close to *Azonexus*_595978, was the most
291 abundant member in all reactors. *Azonexus* is found in partial-denitrification-anammox
292 processes and anaerobic manure digestate and is expected to be involved in N_2O reduction
293 (Huang et al., 2024; Wang et al., 2023). In addition to *Azonexus*, several OTUs close to
294 known N_2O reducers were identified, including *Giesbergeria* (OTU0020) (Zhang et al., 2022),
295 *Thauera*_A_597130 (OTU0013) (Huang et al., 2024), *Denitrificimonas* (OTU0029) (Wang et
296 al., 2024), *Oblitimonas* (OTU0019) (Ramírez-Fernández et al., 2021), and *Sulfurivermis*
297 (OTU0010) (Liu et al., 2023). OTU0020 and OTU0029 were found in reactors with lower
298 N_2O concentrations of 5 and 40 ppm, respectively, whereas OTU0019 was found in reactors
299 with higher N_2O concentrations of 300 ppm and 2,000 ppm. OTU0010 was dominant only in
300 the 2,000 ppm N_2O reactor. Thus, the known N_2O-reducing microorganisms were enriched in
301 the DHS reactors with various concentrations of N_2O.

302 In addition to OTUs close to known N_2O reducers, the relative abundances of many
303 OTUs increased after feeding with N_2O. Although they are not close relatives of N_2O
304 reducers at the genus level, some OTUs belong to the same family as N_2O reducers (e.g.
305 OTU0005 and OTU0009) (Isokpehi et al., 2024). The OTUs increasing the relative
306 abundance could potentially reduce N_2O, although this was difficult to demonstrate using
307 only 16S rRNA gene amplicon analysis.

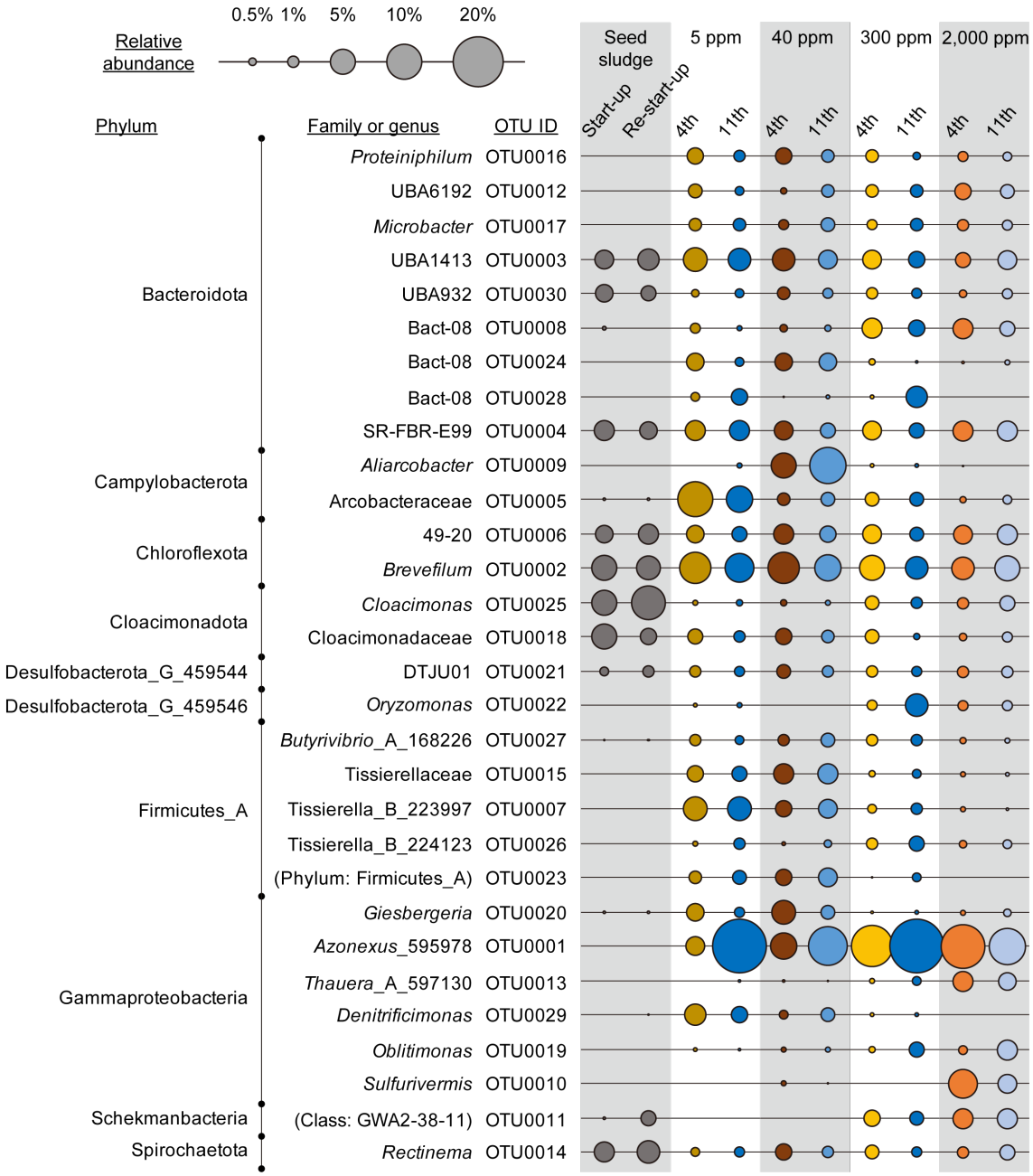

Fig. 3. Top 30 OTUs in the average relative abundance. The size of the circle indicates the relative abundance of OTUs in each sample. 4th: the 4th sponge, 11th: the 11th sponge. Seed sludge: sludge from a mesophilic anaerobic sewage sludge digester.

3.3.2 Metagenome analysis of *nosZ* gene

In total, 229 contigs, including a sequence homologous to *nosZ*, were obtained (matched by BLASTN with sequences longer than approximately 600 bp) (Table S4). The most

317 abundant *nosZ* genes retrieved from all reactors were similar to those in *Azonexus*. In the
318 2,000 ppm N_2O reactor, other than *Azonexus nosZ* gene, *Sulfurivermis*-related *nosZ* gene was
319 obtained in high abundance. This *nosZ* gene was not detected in the other reactors.
320 Additionally, the *Aliarcobacter*-related *nosZ* gene was only found in the 40 ppm N_2O reactor,
321 which was identical to the amplicon analysis (i.e. OTU0009). Besides these microorganisms,
322 *nosZ* gene-harboring microorganisms detected in both 16S rRNA gene amplicons and
323 metagenomic analyses were *Giesbergeria* and *Thauera*.
324 The phylogenetic tree of *nosZ* extracted from metagenomic 229 contigs (Fig. 4) revealed
325 that clade I *nosZ* gene was more diverse and abundant than clade II *nosZ* gene in the reactors.
326 The major N_2O reducers, such as *Azonexus*, *Pseudomonas*_C, *Sulfurivermis, Giesbergeria*
327 and *Thauera,* belong clade I. Clade II *nosZ* genes higher than 1% relative abundance were
328 most obtained from 2,000 ppm N_2O reactor (e.g. *Aequorivit*, *Pelobium*, *Planobacterium*,
329 *Kaistella* and UBA7692). *Aequorivit*-related *nosZ* gene was ranked 4th in relative abundance
330 in the 2,000 ppm N_2O reactor. *Aequorivit* is known not to reduce nitrate (Bowman and
331 Nichols, 2002) and most likely reduce N_2O as a non-denitrifier, which is often found in clade
332 II *nosZ* gene-harbouring microorganisms (Hallin et al., 2018; Sanford et al., 2012). However,
333 many of these known clade II *nosZ* gene harbouring organisms were not detected or less than
334 0.1% in relative abundance, as determined by amplicon analysis.
335

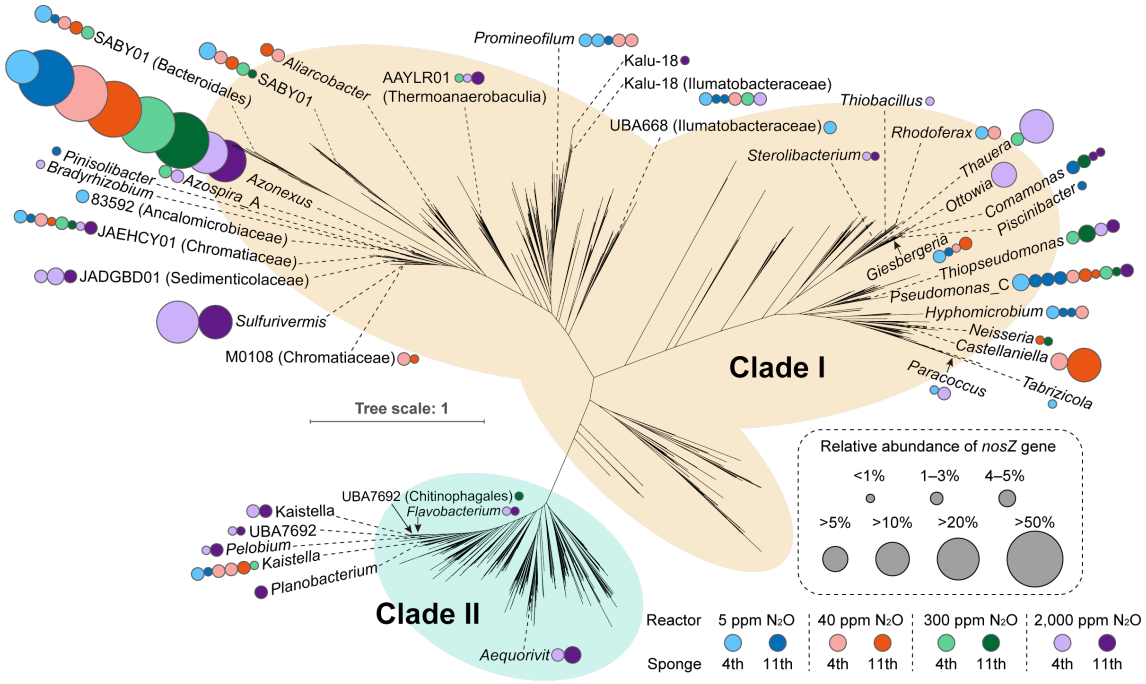

Fig. 4. Phylogenetic tree of NosZ protein. The size of the circles indicates the relative abundance of read counts of contigs with the *nosZ* gene. The colours represent the nitrous oxide concentrations fed to the reactors. 4th: the 4th sponge, 11th: the 11th sponge.

4. Discussion

4.1 Ultra-fast bioprocess for mitigating high concentration N_2O emission

This study demonstrated that the DHS is able to remove N_2O in N_2 gas with removal efficiencies of over 96% for concentrations of up to 300 ppm at 3 min GRT and 2,000 ppm at 18 min GRT with the supply of real wastewater, i.e., the supernatant of sewage sludge digestate. The highest removal rate of 161 ± 26 mg-N/L-reactor/day was achieved when 2,000 ppm N_2O was supplied with a GRT of 9.1 min. One study investigated the removal of N_2O in N_2 gas using a biofilter reactor packed with 2 cm × 2 cm × 2 cm polyurethane cubes (Yoon et al., 2017). This study achieved a removal efficiency of ≥ 99% for 200 ppm N_2O in N_2 gas at GRT of 8.9 min with synthetic wastewater and a removal efficiency of 80–90% at GRT of 32.2 min with wastewater from a primary sedimentation basin treating sewage. Our study demonstrated a much faster treatment (over 10 times) capable of removing higher

353 concentrations of N_2O in N_2 gas compared to that of a previous study, even with the use of
354 real wastewater.
355 High concentrations of N_2O in off-gas were reported, especially from anammox
356 processes, e.g. 0.4–240 ppm (Ali et al., 2016) and 93–1,358 ppm (Okabe et al., 2011) from
357 lab-scale reactors and >4,000 ppm (Kampschreur et al., 2008) from a full-scale reactor
358 although the anammox reaction itself is thought not to produce N_2O (Harris et al., 2015;
359 Kartal et al., 2007). Although the highest concentration tested in this study (i.e., 2,000 ppm)
360 was lower than 4,000 ppm, it showed the potential to remove such high concentrations of N_2O
361 from nitrogen gas. A longer GRT is most probably needed, although a higher removal
362 efficiency can be achieved with a sufficient supply of electron donors, which is directly
363 related to the removal efficiencies of the reactor, as shown in Fig. 2bcd (days 20–50 for the 40,
364 300 and 2,000 ppm reactors).
365 To minimise the amount of N_2O emission from wastewater treatment processes, research
366 focusing solely on N_2O removal efficiency can be misleading. In this study, a removal
367 efficiency of approximately 99% was achieved with a GRT of 18 minutes when 2,000 ppm of
368 N_2O was supplied. However, approximately 20 ppm of N_2O still remained in the off-gas.
369 Particularly in cases where high concentrations of N_2O are treated, implementing an
370 additional treatment process for N_2O removal from the off-gas can further minimise the final
371 N_2O emissions from the process (e.g., a series of DHS reactors).
372
373 **4.2 Kinetics of N_2O reduction in bioreactor**
374 Microelectrode experiments showed an approximately 10-fold faster kinetic potential
375 (Table 1). This suggests that the microbial community inhabiting the reactor had a much
376 greater capacity to reduce N_2O to N_2. Dissolved N_2O was supplied directly to the stirred
377 sludge during the microelectrode experiments (Fig. S1). On the other hand, in the reactor,
378 gaseous N_2O needs to be initially dissolved in the liquid, and then microorganisms can utilise

379 the dissolved N_2O. Thus, the N_2O dissolution rate is the key to determine the removal rate in
380 the reactor.
381 The dissolution rate from gas to liquid can be explained using the Nernst-Noyes-Whitney
382 equation (Dokoumetzidis and Macheras, 2006; Noyes and Whitney, 1897). In the
383 Nernst-Noyes-Whitney equation, the dissolution rate constant (given by the diffusion
384 coefficient of the substance, volume of the solution, and thickness of the diffusion layer),
385 surface area, concentration of the dissolved substance at a given time t, and solubility
386 concentration of the substance were considered. Without N_2O consumption in the liquid phase,
387 the dissolution rate decreases as N_2O dissolves and eventually reaches equilibrium, at which
388 point no more N_2O is removed from the gas phase. However, when microorganisms are
389 present in the liquid phase and actively consume N_2O, the N_2O concentration in the liquid
390 remains low, and the diffusion layer becomes thinner, allowing the dissolution rate to remain
391 high.
392 To achieve faster dissolution rates, it is suggested to increase the surface area of the
393 carrier or enhance the microbial activity to decrease the dissolved N_2O concentration in the
394 liquid phase and reduce the thickness of the diffusion layer. One could consider supplying
395 different substrates utilised by other microorganisms to enhance microbial activity to enable
396 faster N_2O reduction. An earlier study (Yoon et al., 2017) reported a higher N_2O removal
397 efficiency with synthetic wastewater than that with real wastewater, i.e., effluent from a
398 primary sedimentation basin treating sewage. Additionally, increasing the temperature would
399 help accelerate the microbial N_2O reduction rate and increase the diffusion coefficient.
400
401 **4.3 Nitrous oxide reducers in bioreactors**
402 Sludge from the sponges in each reactor was collected on the last day of operation and
403 subjected to 16S rRNA amplicon sequencing analysis. A comparison of the microbial
404 community structure based on PCoA (Fig. S2) showed that the microbial communities in the

405 N_2O-reducing DHS reactors were different from those in the seed sludge, i.e., sludge from an
406 anaerobic sewage sludge digester, as well as those in the supernatant of an anaerobic sludge
407 digestate, i.e., the substrate for denitrification. It also showed a change in the microbial
408 community under different N_2O concentrations, as well as in the height of the reactor (Figs. 3
409 and S2). In a DHS reactor, COD load changes along the height (Kubota et al., 2014), i.e.,
410 higher and lower COD concentrations occur in the upper and lower part of the reactor,
411 respectively. Additionally, the supernatant of the anaerobic sludge digestate contains diverse
412 electron donors. These characteristics provide a habitat for a variety of microorganisms in the
413 reactors compared with that of earlier studies using a simple substrate for N_2O reduction (e.g.,
414 acetate for Conthe et al. 2018).

415 In the N_2O reducing DHS reactors, *Azonexus* was the most abundant genus after both
416 amplicon and metagenome analyses (Fig. 3 and Table S4). *Azonexus* can utilise intermediates
417 of anaerobic organic degradation such as acetate and propionate (Quan et al., 2006). The
418 digestate supernatant contained a small number of fatty acids. Additionally, the substrate may
419 be anaerobically degraded in the reactor, and the intermediates may be used by *Azonexus* as
420 carbon sources to reduce N_2O. An earlier study detected *Azonexus* in a bioreactor
421 continuously supplying N_2O and acetate under anaerobic conditions (Conthe et al., 2018).
422 Thus, *Azonexus* plays a key role in N_2O removal.

423 Other than *Azonexus*, *Sulfurivermis*, which can also utilise acetate and propionate for
424 nitrate reduction (Watanabe et al., 2019), was found to be the second most abundant
425 denitrifier, with high relative abundance (26% in the 4th sponge and 17% in the 11th sponge)
426 in the 2,000 ppm reactor. Additionally, *Aliarcobacter* was found in the 40 ppm N_2O reactor.
427 Because a slightly larger sponge medium (30 mm in diameter and 30 mm in height) was used,
428 a gradient of dissolved N_2O concentration occurred in the sponge media, which may have
429 involved a variety of microorganisms in N_2O reduction.

430 The *nosZ* genes retrieved from the reactors showed that clade I *nosZ* was more
431 predominant and diverse than clade II *nosZ* (Fig. 4). All the top three relatively abundant *nosZ*
432 genes belonged to clade I and only a small number of clade II *nosZ* genes were obtained with
433 low relative abundance. A higher number of clade II *nosZ* genes were obtained from the 2,000
434 ppm N_2O reactor. Generally, microorganisms that possess the clade II *nosZ* gene have lower
435 half-saturation constant (K_m) values and higher affinity than clade I N_2O-reducing
436 microorganisms and are more abundant in environments where low concentrations of N_2O are
437 available (Suenaga et al., 2018; Yoon et al., 2016). This suggests that niche
438 compartmentalisation of clade I N_2O-reduers and clade II N_2O-reducers may exist in sponge
439 media. Faster-growing-and-low-affinity microorganisms (i.e. those with clade I *nosZ* genes,
440 such as *Azonexus*) may be present in the outer layer of the sponge, whereas
441 slow-growing-and-high-affinity microorganisms (i.e. those with clade II *nosZ* genes) may be
442 present in the inner part of the sponge. In the 2,000 ppm N_2O reactor, the concentration
443 gradient of dissolved N_2O may have occurred deeper in the sponge, resulting in a more
444 suitable environment for those harbouring the clade II *nosZ* gene.
445
446 **5. Conclusion**
447 In this study, a novel ultra-fast N_2O removal process using a DHS reactor was
448 developed to remove high concentrations of N_2O generated from anaerobic/anoxic wastewater
449 treatment processes such as an anammox process. Continuous experiments revealed that more
450 than 96% removal rates were achieved for up to 300 ppm N_2O gas with 3 min GRT and 2,000
451 ppm N_2O with 18 min GRT. The maximum N_2O removal rate of 161 ± 26
452 mg-N/L-reactor/day was obtained when 2,000 ppm N_2O was supplied with the GRT of 9.1
453 min, which is over 10 times faster than the pioneering process. Additionally, the lack of
454 organic supply immediately deteriorates the N_2O removal performance. Kinetic analysis
455 indicated that the N_2O dissolution rate is a crucial factor in determining the N_2O removal rate

456 in the reactor. Amplicon and metagenome analyses showed that *Azonexus* played a key role in
457 N_2O removal. A gradient of dissolved N_2O concentration may occur in the sponge carriers,
458 resulting in the involvement of various microorganisms in N_2O reduction. Most of the *nosZ*
459 genes obtained from the reactors belonged to clade I and only a few fractions were clade II
460 *nosZ* genes, suggesting the possibility of niche compartmentalisation between clade I
461 N_2O-reducers and clade II N_2O-reduers in the sponge with gradient of dissolved N_2O
462 concentrations.
463

464 **Acknowledgements**

465 This study was supported by KAKENHI grants (JP19KK0371, JP21H01460) from the Japan
466 Society for the Promotion of Science (JSPS), the Moonshot project JPNP18016,
467 commissioned by the New Energy and Industrial Technology Development Organization
468 (NEDO) and the MEXT WISE Program for Sustainability in Dynamic Earth (SyDE), Japan.
469 RM was supported by a Grant-in-Aid for JSPS Fellows (JP24KJ0429).
470

471 **References**

472 Ali, M., Rathnayake, R.M.L.D., Zhang, L., Ishii, S., Kindaichi, T., Satoh, H., Toyoda, S.,
473 Yoshida, N., Okabe, S., 2016. Source identification of nitrous oxide emission pathways
474 from a single-stage nitritation-anammox granular reactor. Water Res. 102, 147–157.
475 https://doi.org/10.1016/j.watres.2016.06.034
476 Altschul, S.F., Gish, W., Miller, W., Myers, E.W., Lipman, D.J., 1990. Basic Local
477 Alignment Search Tool. J. Mol. Biol. 215, 403–410.
478 APHP, 2017. Standard methods for the examination of water and wastewater, 23rd ed,
479 American Public Health Association,Washington DC.

480 Aroney, S.T.N., Newell, R.J.P., Nissen, J., Camargo, A.P., Tyson, G.W., Woodcroft, B.J.,
481 2024. CoverM: Read coverage calculator for metagenomics (v0.7.0). Zenodo.
482 https://doi.org/10.5281/zenodo.10531254
483 Bolyen, E., Rideout, J.R., Dillon, M.R., Bokulich, N.A., Abnet, C.C., Al-Ghalith, G.A.,
484 Alexander, H., Alm, E.J., Arumugam, M., Asnicar, F., Bai, Y., Bisanz, J.E., Bittinger, K.,
485 Brejnrod, A., Brislawn, C.J., Brown, C.T., Callahan, B.J., Caraballo-Rodríguez, A.M.,
486 Chase, J., Cope, E.K., Da Silva, R., Diener, C., Dorrestein, P.C., Douglas, G.M., Durall,
487 D.M., Duvallet, C., Edwardson, C.F., Ernst, M., Estaki, M., Fouquier, J., Gauglitz, J.M.,
488 Gibbons, S.M., Gibson, D.L., Gonzalez, A., Gorlick, K., Guo, J., Hillmann, B., Holmes,
489 S., Holste, H., Huttenhower, C., Huttley, G.A., Janssen, S., Jarmusch, A.K., Jiang, L.,
490 Kaehler, B.D., Kang, K. Bin, Keefe, C.R., Keim, P., Kelley, S.T., Knights, D., Koester,
491 I., Kosciolek, T., Kreps, J., Langille, M.G.I., Lee, J., Ley, R., Liu, Y.X., Loftfield, E.,
492 Lozupone, C., Maher, M., Marotz, C., Martin, B.D., McDonald, D., McIver, L.J., Melnik,
493 A. V., Metcalf, J.L., Morgan, S.C., Morton, J.T., Naimey, A.T., Navas-Molina, J.A.,
494 Nothias, L.F., Orchanian, S.B., Pearson, T., Peoples, S.L., Petras, D., Preuss, M.L.,
495 Pruesse, E., Rasmussen, L.B., Rivers, A., Robeson, M.S., Rosenthal, P., Segata, N.,
496 Shaffer, M., Shiffer, A., Sinha, R., Song, S.J., Spear, J.R., Swafford, A.D., Thompson,
497 L.R., Torres, P.J., Trinh, P., Tripathi, A., Turnbaugh, P.J., Ul-Hasan, S., van der Hooft,
498 J.J.J., Vargas, F., Vázquez-Baeza, Y., Vogtmann, E., von Hippel, M., Walters, W., Wan,
499 Y., Wang, M., Warren, J., Weber, K.C., Williamson, C.H.D., Willis, A.D., Xu, Z.Z.,
500 Zaneveld, J.R., Zhang, Y., Zhu, Q., Knight, R., Caporaso, J.G., 2019. Reproducible,
501 interactive, scalable and extensible microbiome data science using QIIME 2. Nat.
502 Biotechnol. 37, 852–857. https://doi.org/10.1038/s41587-019-0209-9
503 Bowman, J.P., Nichols, D.S., 2002. Aequorivita gen. nov., a member of the family
504 Flavobacteriaceae isolated from terrestrial and marine Antarctic habitats. Int. J. Syst.
505 Evol. Microbiol. 52, 1533–1541. https://doi.org/10.1099/ijs.0.01976-0.The

506 Callahan, B.J., McMurdie, P.J., Rosen, M.J., Han, A.W., Johnson, A.J.A., Holmes, S.P., 2016.
507 DADA2: High-resolution sample inference from Illumina amplicon data. Nat. Methods
508 13, 581–583. https://doi.org/10.1038/nmeth.3869
509 Capella-Gutiérrez, S., Silla-Martínez, J.M., Gabaldón, T., 2009. trimAl: A tool for automated
510 alignment trimming in large-scale phylogenetic analyses. Bioinformatics 25, 1972–1973.
511 https://doi.org/10.1093/bioinformatics/btp348
512 Chen, Yuxin, Chen, Yongsheng, Shi, C., Huang, Z., Zhang, Y., Li, S., Li, Y., Ye, J., Yu, C.,
513 Li, Z., Zhang, X., Wang, J., Yang, H., Fang, L., Chen, Q., 2018. SOAPnuke: A
514 MapReduce acceleration-supported software for integrated quality control and
515 preprocessing of high-throughput sequencing data. Gigascience 7, 1–6.
516 https://doi.org/10.1093/gigascience/gix120
517 Conthe, M., Wittorf, L., Kuenen, J.G., Kleerebezem, R., Van Loosdrecht, M.C.M., Hallin, S.,
518 2018. Life on N_2O: Deciphering the ecophysiology of N_2O respiring bacterial
519 communities in a continuous culture. ISME J. 12, 1142–1153.
520 https://doi.org/10.1038/s41396-018-0063-7
521 Dokoumetzidis, A., Macheras, P., 2006. A century of dissolution research: From Noyes and
522 Whitney to the Biopharmaceutics Classification System. Int. J. Pharm. 321, 1–11.
523 https://doi.org/10.1016/j.ijpharm.2006.07.011
524 Domingo-Félez, C., Smets, B.F., 2019. Regulation of key N_2O production mechanisms during
525 biological water treatment. Curr. Opin. Biotechnol. 57, 119–126.
526 https://doi.org/10.1016/j.copbio.2019.03.006
527 Duan, H., Zhao, Y., Koch, K., Wells, G.F., Zheng, M., Yuan, Z., Ye, L., 2021. Insights into
528 Nitrous Oxide Mitigation Strategies in Wastewater Treatment and Challenges for Wider
529 Implementation. Environ. Sci. Technol. 55, 7208–7224.
530 https://doi.org/10.1021/acs.est.1c00840

Frutos, O.D., Quijano, G., Pérez, R., Muñoz, R., 2016. Simultaneous biological nitrous oxide abatement and wastewater treatment in a denitrifying off-gas bioscrubber. Chem. Eng. J. 288, 28–37. https://doi.org/10.1016/j.cej.2015.11.088

Hallin, S., Philippot, L., Löffler, F.E., Sanford, R.A., Jones, C.M., 2018. Genomics and Ecology of Novel N2O-Reducing Microorganisms. Trends Microbiol. 26, 43–55. https://doi.org/10.1016/j.tim.2017.07.003

Han, H., Kim, D.D., Song, M.J., Yun, T., Yoon, H., Lee, H.W., Kim, Y.M., Laureni, M., Yoon, S., 2023. Biotrickling Filtration for the Reduction of N_2O Emitted during Wastewater Treatment: Results from a Long-Term In Situ Pilot-Scale Testing. Environ. Sci. Technol. 57, 3883–3892. https://doi.org/10.1021/acs.est.2c08818

Harris, E., Joss, A., Emmenegger, L., Kipf, M., Wolf, B., Mohn, J., Wunderlin, P., 2015. Isotopic evidence for nitrous oxide production pathways in a partial nitritation-anammox reactor. Water Res. 83, 258–270. https://doi.org/10.1016/j.watres.2015.06.040

Hu, Z., Zhang, J., Xie, H., Liang, S., Li, S., 2013. Minimization of nitrous oxide emission from anoxic-oxic biological nitrogen removal process: Effect of influent COD/NH_4^+ ratio and feeding strategy. J. Biosci. Bioeng. 115, 272–278. https://doi.org/10.1016/j.jbiosc.2012.09.016

Huang, K., He, Y., Wang, W., Jiang, R., Zhang, Y., Li, J., Zhang, X.X., Wang, D., 2024. Temporal differentiation in the adaptation of functional bacteria to low-temperature stress in partial denitrification and anammox system. Environ. Res. 244, 117933. https://doi.org/10.1016/j.envres.2023.117933

IPCC, 2022. Summary for Policymakers. In: Climate Change 2022: Mitigation of Climate Change, Cambridge University Press. https://doi.org/10.1017/9781009157926.001

Isokpehi, R.D., Kim, Y., Krejci, S.E., Trivedi, V.D., 2024. Ecological Trait-Based Digital Categorization of Microbial Genomes for Denitrification Potential. Microorganisms 12, 791. https://doi.org/10.3390/microorganisms12040791

557 Kalyaanamoorthy, S., Minh, B.Q., Wong, T.K.F., Von Haeseler, A., Jermiin, L.S., 2017.
558 ModelFinder: Fast model selection for accurate phylogenetic estimates. Nat. Methods 14,
559 587–589. https://doi.org/10.1038/nmeth.4285
560 Kampschreur, M.J., Temmink, H., Kleerebezem, R., Jetten, M.S.M., van Loosdrecht, M.C.M.,
561 2009. Nitrous oxide emission during wastewater treatment. Water Res. 43, 4093–4103.
562 https://doi.org/10.1016/j.watres.2009.03.001
563 Kampschreur, M.J., van der Star, W.R.L., Wielders, H.A., Mulder, J.W., Jetten, M.S.M., van
564 Loosdrecht, M.C.M., 2008. Dynamics of nitric oxide and nitrous oxide emission during
565 full-scale reject water treatment. Water Res. 42, 812–826.
566 https://doi.org/10.1016/j.watres.2007.08.022
567 Kartal, B., Kuypers, M.M.M., Lavik, G., Schalk, J., Op Den Camp, H.J.M., Jetten, M.S.M.,
568 Strous, M., 2007. Anammox bacteria disguised as denitrifiers: Nitrate reduction to
569 dinitrogen gas via nitrite and ammonium. Environ. Microbiol. 9, 635–642.
570 https://doi.org/10.1111/j.1462-2920.2006.01183.x
571 Katoh, K., Misawa, K., Kuma, K.I., Miyata, T., 2002. MAFFT: A novel method for rapid
572 multiple sequence alignment based on fast Fourier transform. Nucleic Acids Res. 30,
573 3059–3066. https://doi.org/10.1093/nar/gkf436
574 Kubota, K., Hayashi, M., Matsunaga, K., Iguchi, A., Ohashi, A., Li, Y.Y., Yamaguchi, T.,
575 Harada, H., 2014. Microbial community composition of a down-flow hanging sponge
576 (DHS) reactor combined with an up-flow anaerobic sludge blanket (UASB) reactor for
577 the treatment of municipal sewage. Bioresour. Technol. 151, 144–150.
578 https://doi.org/10.1016/j.biortech.2013.10.058
579 Kubota, K., Otani, T., Hariu, T., Jin, T., Tagawa, T., Morikawa, M., Li, Y.Y., 2024.
580 Evaluation of sewage treatment performance and duckweed biomass production
581 efficiency in a primary sedimentation basin + duckweed pond + downflow hanging

582 sponge (PSB + DWP + DHS) system. J. Water Process Eng. 65, 105818.
583 https://doi.org/10.1016/j.jwpe.2024.105818
584 Lackner, S., Gilbert, E.M., Vlaeminck, S.E., Joss, A., Horn, H., van Loosdrecht, M.C.M.,
585 2014. Full-scale partial nitritation/anammox experiences – An application survey. Water
586 Res. 55, 292–303. https://doi.org/10.1016/j.watres.2014.02.032
587 Letunic, I., Bork, P., 2021. Interactive tree of life (iTOL) v5: An online tool for phylogenetic
588 tree display and annotation. Nucleic Acids Res. 49, W293–W296.
589 https://doi.org/10.1093/nar/gkab301
590 Liu, P., Zou, S., Zhang, H., Liu, Q., Song, Z., Huang, Y., Hu, X., 2023. Genome-resolved
591 metagenomics provides insights into the microbial-mediated sulfur and nitrogen cycling
592 in temperate seagrass meadows. Front. Mar. Sci. 10, 1245288.
593 https://doi.org/10.3389/fmars.2023.1245288
594 Matsubayashi, M., Shimada, Y., Li, Y.Y., Harada, H., Kubota, K., 2017. Phylogenetic
595 diversity and in situ detection of eukaryotes in anaerobic sludge digesters. PLoS One
596 12, e0172888. https://doi.org/10.1371/journal.pone.0172888
597 McDonald, D., Jiang, Y., Balaban, M., Cantrell, K., Zhu, Q., Gonzalez, A., Morton, J.T.,
598 Nicolaou, G., Parks, D.H., Karst, S.M., Albertsen, M., Hugenholtz, P., DeSantis, T.,
599 Song, S.J., Bartko, A., Havulinna, A.S., Jousilahti, P., Cheng, S., Inouye, M., Niiranen,
600 T., Jain, M., Salomaa, V., Lahti, L., Mirarab, S., Knight, R., 2023. Greengenes2 unifies
601 microbial data in a single reference tree. Nat. Biotechnol. 42, 715–718.
602 https://doi.org/10.1038/s41587-023-01845-1
603 Minh, B.Q., Schmidt, H.A., Chernomor, O., Schrempf, D., Woodhams, M.D., Von Haeseler,
604 A., Lanfear, R., Teeling, E., 2020. IQ-TREE 2: New Models and Efficient Methods for
605 Phylogenetic Inference in the Genomic Era. Mol. Biol. Evol. 37, 1530–1534.
606 https://doi.org/10.1093/molbev/msaa015

607 Newell, R.J.P., Aroney, S.T.N., Zaugg, J., Sternes, P., Tyson, G.W., Woodcroft, B.J., 2023.
608 Aviary : Hybrid assembly and genome recovery from metagenomes with Aviary (v0.8.3).
609 Zenodo. https://doi.org/10.5281/zenodo.10158086.
610 Ni, J., Hatori, S., Wang, Y., Li, Y.Y., Kubota, K., 2020. Uncovering Viable Microbiome in
611 Anaerobic Sludge Digesters by Propidium Monoazide (PMA)-PCR. Microb. Ecol. 79,
612 925–932. https://doi.org/10.1007/s00248-019-01449-w
613 Noyes, A.A., Whitney, W.R., 1897. The rate of solution of solid substances in their own
614 solutions. J. Am. Chem. Soc. 19, 930–934.
615 Oba, K., Suenaga, T., Yasuda, S., Kuroiwa, M., Hori, T., Lackner, S., Terada, A., 2024. Quest
616 for Nitrous Oxide-reducing Bacteria Present in an Anammox Biofilm Fed with Nitrous
617 Oxide. Microbes Environ. 39, ME23106. https://doi.org/10.1264/jsme2.ME23106
618 Okabe, S., Oshiki, M., Takahashi, Y., Satoh, H., 2011. N_2O emission from a partial
619 nitrification-anammox process and identification of a key biological process of N2O
620 emission from anammox granules. Water Res. 45, 6461–6470.
621 https://doi.org/10.1016/j.watres.2011.09.040
622 Peng, L., Carvajal-Arroyo, J.M., Seuntjens, D., Prat, D., Colica, G., Pintucci, C., Vlaeminck,
623 S.E., 2017. Smart operation of nitritation/denitritation virtually abolishes nitrous oxide
624 emission during treatment of co-digested pig slurry centrate. Water Res. 127, 1–10.
625 https://doi.org/10.1016/j.watres.2017.09.049
626 Quan, Z.X., Im, W.T., Lee, S.T., 2006. *Azonexus caeni* sp. nov., a denitrifying bacterium
627 isolated from sludge of a wastewater treatment plant. Int. J. Syst. Evol. Microbiol. 56,
628 1043–1046. https://doi.org/10.1099/ijs.0.64019-0
629 Ramírez-Fernández, L., Orellana, L.H., Johnston, E.R., Konstantinidis, K.T., Orlando, J.,
630 2021. Diversity of microbial communities and genes involved in nitrous oxide emissions
631 in Antarctic soils impacted by marine animals as revealed by metagenomics and 100

632 metagenome-assembled genomes. Sci. Total Environ. 788, 147693.
633 https://doi.org/10.1016/j.scitotenv.2021.147693
634 Ravishankara, A.R., Daniel, J.S., Portmann, R.W., 2009. Nitrous oxide (N_2O): The dominant
635 ozone-depleting substance emitted in the 21st century. Science 326, 123–125.
636 https://doi.org/10.1126/science.1176985
637 Rognes, T., Flouri, T., Nichols, B., Quince, C., Mahé, F., 2016. VSEARCH: A versatile open
638 source tool for metagenomics. PeerJ 4, e2584. https://doi.org/10.7717/peerj.2584
639 Sabba, F., Terada, A., Wells, G., Smets, B.F., Nerenberg, R., 2018. Nitrous oxide emissions
640 from biofilm processes for wastewater treatment. Appl. Microbiol. Biotechnol. 102,
641 9815–9829. https://doi.org/10.1007/s00253-018-9332-7
642 Sanford, R.A., Wagner, D.D., Wu, Q., Chee-Sanford, J.C., Thomas, S.H., Cruz-García, C.,
643 Rodríguez, G., Massol-Deyá, A., Krishnani, K.K., Ritalahti, K.M., Nissen, S.,
644 Konstantinidis, K.T., Löffler, F.E., 2012. Unexpected nondenitrifier nitrous oxide
645 reductase gene diversity and abundance in soils. Proc. Natl. Acad. Sci. U. S. A. 109,
646 19709–19714. https://doi.org/10.1073/pnas.1211238109
647 Seemann, T., 2014. Prokka: Rapid prokaryotic genome annotation. Bioinformatics 30,
648 2068–2069. https://doi.org/10.1093/bioinformatics/btu153
649 Suenaga, T., Riya, S., Hosomi, M., Terada, A., 2018. Biokinetic characterization and
650 activities of N_2O-reducing bacteria in response to various oxygen levels. Front.
651 Microbiol. 9, 697. https://doi.org/10.3389/fmicb.2018.00697
652 Tanikawa, D., Motokawa, D., Itoiri, Y., Kimura, Z.I., Ito, M., Nagano, A., 2022. Biogas
653 purification and ammonia load reduction in sewage treatment by two-stage down-flow
654 hanging sponge reactor. Sci. Total Environ. 851, 158355.
655 https://doi.org/10.1016/j.scitotenv.2022.158355
656 Tian, H., Xu, R., Canadell, J.G., Thompson, R.L., Winiwarter, W., Suntharalingam, P.,
657 Davidson, E.A., Ciais, P., Jackson, R.B., Janssens-Maenhout, G., Prather, M.J., Regnier,

P., Pan, N., Pan, S., Peters, G.P., Shi, H., Tubiello, F.N., Zaehle, S., Zhou, F., Arneth, A., Battaglia, G., Berthet, S., Bopp, L., Bouwman, A.F., Buitenhuis, E.T., Chang, J., Chipperfield, M.P., Dangal, S.R.S., Dlugokencky, E., Elkins, J.W., Eyre, B.D., Fu, B., Hall, B., Ito, A., Joos, F., Krummel, P.B., Landolfi, A., Laruelle, G.G., Lauerwald, R., Li, W., Lienert, S., Maavara, T., MacLeod, M., Millet, D.B., Olin, S., Patra, P.K., Prinn, R.G., Raymond, P.A., Ruiz, D.J., van der Werf, G.R., Vuichard, N., Wang, J., Weiss, R.F., Wells, K.C., Wilson, C., Yang, J., Yao, Y., 2020. A comprehensive quantification of global nitrous oxide sources and sinks. Nature 586, 248–256. https://doi.org/10.1038/s41586-020-2780-0

Vasilaki, V., Massara, T.M., Stanchev, P., Fatone, F., Katsou, E., 2019. A decade of nitrous oxide (N_2O) monitoring in full-scale wastewater treatment processes: A critical review. Water Res. 161, 392–412. https://doi.org/10.1016/j.watres.2019.04.022

Wang, S., Yuan, C., Xu, C., Li, D., Zhang, H., Wang, J., Wang, X., Li, Y., Jiao, D., Yuan, S., Chen, H., Qiu, D., 2024. Denitrificimonas halotolerans sp. nov., a novel species isolated from UASB sludge treating landfill leachate. Antonie van Leeuwenhoek, Int. J. Gen. Mol. Microbiol. 117, 91. https://doi.org/10.1007/s10482-024-01987-5

Wang, X., Xiang, B., Li, J., Zhang, M., Frostegard, A., Bakken, L., Zhang, X., 2023. Using adaptive and aggressive N_2O-reducing bacteria to augment digestate fertilizer for mitigating N_2O emissions from agricultural soils. Sci. Total Environ. 903, 166284. https://doi.org/10.1016/j.scitotenv.2023.166284

Watanabe, T., Kojima, H., Umezawa, K., Hori, C., Takasuka, T.E., Kato, Y., Fukui, M., 2019. Genomes of neutrophilic sulfur-oxidizing chemolithoautotrophs representing 9 proteobacterial species from 8 genera. Front. Microbiol. 10, 00316. https://doi.org/10.3389/fmicb.2019.00316

Wu, L., Peng, L., Wei, W., Wang, D., Ni, B.J., 2020. Nitrous oxide production from wastewater treatment: The potential as energy resource rather than potent greenhouse gas. J. Hazard. Mater. 387, 121694. https://doi.org/10.1016/j.jhazmat.2019.121694

Yamaguchi, Tsuyoshi, Nakamura, S., Hatamoto, M., Tamura, E., Tanikawa, D., Kawakami, S., Nakamura, A., Kato, K., Nagano, A., Yamaguchi, Takashi, 2018. A novel approach for toluene gas treatment using a downflow hanging sponge reactor. Appl. Microbiol. Biotechnol. 102, 5625–5634. https://doi.org/10.1007/s00253-018-8933-5

Yoon, H., Song, M.J., Kim, D.D., Sabba, F., Yoon, S., 2019. A Serial Biofiltration System for Effective Removal of Low-Concentration Nitrous Oxide in Oxic Gas Streams: Mathematical Modeling of Reactor Performance and Experimental Validation. Environ. Sci. Technol. 53, 2063–2074. https://doi.org/10.1021/acs.est.8b05924

Yoon, H., Song, M.J., Yoon, S., 2017. Design and Feasibility Analysis of a Self-Sustaining Bio fi ltration System for Removal of Low Concentration N2O Emitted from Wastewater Treatment Plants. https://doi.org/10.1021/acs.est.7b02750

Yoon, S., Nissen, S., Park, D., Sanford, R.A., Löffler, E., 2016. Clade I NosZ from Those Harboring Clade II NosZ. Appl. Envioronmental Microbiol. 82, 3793–3800. https://doi.org/10.1128/AEM.00409-16.Editor

Zhang, Z., Zhang, Y., Shi, Z., Chen, Y., 2022. Linking Genome-Centric Metagenomics to Kinetic Analysis Reveals the Regulation Mechanism of Hydroxylamine in Nitrite Accumulation of Biological Denitrification. Environ. Sci. Technol. 56, 10317–10328. https://doi.org/10.1021/acs.est.2c01914

Zheng, X., Yan, Z., Zhao, C., He, L., Lin, Z., Liu, M., 2023. Homogeneous environmental selection mainly determines the denitrifying bacterial community in intensive aquaculture water. Front. Microbiol. 14, 1280450. https://doi.org/10.3389/fmicb.2023.1280450